Available online at www.sciencedirect.com
ScienceDirect
Journal of Power Sources 178 (2008) 852–856
JOURNAL OF POWER SOURCES
www.elsevier.com/locate/jpowsour

Short communication

The discharge properties of Na/Ni_3S_2 cell at ambient temperature

Jong-Seon Kim [a], Hyo-Jun Ahn [a,*], Ho-Suk Ryu [a], Dong-Ju Kim [a], Gyu-Bong Cho [a], Ki-Won Kim [a], Tae-Hyun Nam [a], Jou Hyeon Ahn [b]

[a] *i-Cube Center, ReCAPT, Nano and Advanced Materials Engineering, Gyeongsang National University, 900 Gajwadong, Jinju, Gyeongnam 660-701, Republic of Korea*
[b] *Department of Chemical & Biological Engineering, Gyeongsang National University, 900 Gajwadong, Jinju, Gyeongnam 660-701, Republic of Korea*

Received 30 June 2007; received in revised form 19 September 2007; accepted 24 September 2007
Available online 29 September 2007

Abstract

The discharge properties of a Na/Ni_3S_2 cell using 1 M $NaCF_3SO_3$ in tetra(ethylene glycol)dimethyl ether liquid electrolyte were investigated at room temperature. The products were characterized by X-ray diffraction, scanning electron microscopy and energy dispersive spectroscopy. Electrochemical properties of Na/Ni_3S_2 cells were also presented by cyclic voltammetry and the galvanostatic current method. Na/Ni_3S_2 cells have an initial discharge capacity of 420 mAh g^{-1} with a plateau potential at 0.94 V versus Na/Na^+. After the first discharge, Ni_3S_2 and Na react at room temperature and then form sodium sulfide (Na_2S) and nickel. Sodium ion can be partially deintercalated from Na_2S charge reaction. The discharge process can be explained as follows: $Ni_3S_2 + 4Na \leftrightarrow 3Ni + 2Na_2S$.

Keywords: Sodium battery; Nickel sulfide cathode; Na/Ni_3S_2 cell; Discharge property

1. Introduction

Because of the high-price of oil and environmental pollution, electric vehicles (EV) and hybrid electric vehicles (HEV) have received increasing attention in recent years. Many battery systems have been studied as power sources of EV or HEV. These battery systems demand a high-specific energy density, a high-specific power, low material cost, and a long cycle life. Ni/MH batteries offer superior performance, reliability, and safety, and are already commercialized [1]. Li ion batteries are researched extensively for large-scale EV and HEV [2].

The sodium/sulfur cell at a high-temperature might be a good candidate for EV or HEV because of a high-theoretical specific energy density of 760 W kg^{-1}, low-cost, high power density, and long cycle life [3]. However a sodium/sulfur cell could be operated above 300 °C to ensure sufficient sodium ion conductivity in a solid electrolyte. At this operation temperature, both sulfur and sodium are in the liquid state, which might induce a leakage of liquid materials, an explosion, or corrosion by sodium polysulfides [4]. Safety was an important issue for sodium/sulfur cells [3]. Several groups [5,6] began to develop sodium batteries operating at room temperature. The sodium and sulfur are solid state at room temperature, which is safer than a liquid state. However Na/S batteries have a poor cycle life [5–7].

Among the various candidates for cathode materials, the nickel sulfides show a high-theoretical capacity and long cycle life [8–10]. Also, since nickel sulfides exist in nature as minerals such as heazelwoodite (Ni_3S_2), Ni_3S_2 is abundant and cheap. Jasinski and Burrows [11] reported that lithium/nickel sulfides cells showed high utilization in 1 M $LiClO_4$ in propylene carbonate (PC). Although Ni_3S_2 is a potential cathode material for the sodium battery system, a study of Na/Ni_3S_2 cells has never been reported.

In this paper, a Na/Ni_3S_2 cell was prepared and the electrochemical properties of the cells were investigated at ambient temperature. The discharge mechanism was discussed from the discharge curves, SEM, XRD, and EDS data.

2. Experimental

Nickel sulfide (Ni_3S_2) powders were bought from Aldrich Chemical Co. In order to decrease a particle size of Ni_3S_2

* Corresponding author. Tel.: +82 55 751 5308; fax: +82 55 759 1745.
E-mail address: ahj@gnu.ac.kr (H.-J. Ahn).

0378-7753/$ – see front matter © 2007 Elsevier B.V. All rights reserved.
doi:10.1016/j.jpowsour.2007.09.067

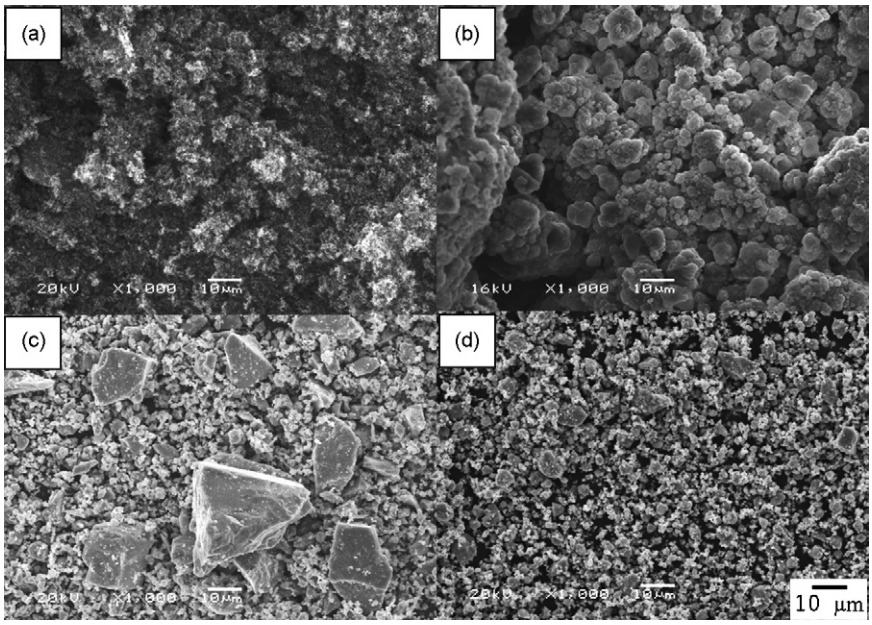

Fig. 1. SEM morphologies of raw materials: (a) carbon, (b) PEO, (c) raw Ni_3S_2, and (d) Ni_3S_2 after ball-milling for 2 h.

(−150 mesh) powder, a planetary ball-milling (FRITSCH Co.) was executed for 2 h. Carbon black (Super-P, MMM Carbon) dried in an oven at 80 °C and poly ethylene oxide (PEO, $(–CH_2CH_2O)_n$, Aldrich Chem. Co.) was used without pretreatment.

The cathode (Ni_3S_2) slurry was prepared by mixing Ni_3S_2 powder (60 wt.%), PEO (20 wt.%) and Super-P (20 wt.%) in acetonitrile (ACN, Aldrich Chem. Co., 99.5%). The slurry was mixed homogeneously by a planetary ball-milling for 3 h. The homogeneous slurry was coated onto an aluminum foil current collector using a doctor blade method. In order to remove solvent and volatile impurities, the slurry was dried at 60 °C for a day and then at 50 °C for 5 h under a vacuum atmosphere. The dried cathode film was cut into disc shapes of 1.0 cm diameter. The cell was fabricated using sodium slices (Aldrich Chem. Co.) as an anode, a porous polypropylene film (Cellgard®-2400) as a separator, and used 1 M sodium trifluoromethanesulfonate ($NaCF_3SO_3$, Aldrich Chem. Co.) salt in tetra(ethylene glycol)dimethyl ether (TEGDME, Aldrich Chem. Co.) as an electrolyte. The cell was assembled in a glove box with an argon atmosphere.

The electrochemical tests were performed by WBCS 3000 Battery Tester (WonA Tech) at room temperature. The Na/Ni_3S_2 cells were discharged and charged galvanostatically at voltage from 0.4 to 2.6 V. The cyclic voltammogram of a Na/Ni_3S_2 cell is performed with a scan rate of 0.1 mV s^{-1}. In order to confirm products during the charge–discharge reaction, X-ray diffraction (XRD, D8 Discover, Bruker AXS) patterns were obtained using Cu Kα radiation. Scanning electron microscopy (SEM, JEOL JSM 5600) was employed to observe the surface morphology. Elemental mapping of the electrode was measured using an energy dispersive spectrometer (EDS, INCA Energy, Oxford Instruments).

3. Results and discussion

Fig. 1 shows SEM morphologies of raw materials which are conductive carbon, PEO, Ni_3S_2 powders, and Ni_3S_2 powder after ball-milling for 2 h. Carbon particles have a submicrometer diameter and very large surface areas. PEO particles were agglomerated with small particles. When the Ni_3S_2 powder was purchased from the Aldrich Company, some of the Ni_3S_2 powders have a larger size. The particle size of Ni_3S_2 powders decreased below 10 μm after ball-milling for 2 h.

The X-ray diffraction patterns of the raw materials are presented in Fig. 2. Carbon shows two broad peaks, which can be related to a nanocrystalline structure. The sharp peak of PEO indicates a crystalline structure. The majority of the XRD peaks for the original Ni_3S_2 powders are coincided with the rhom-

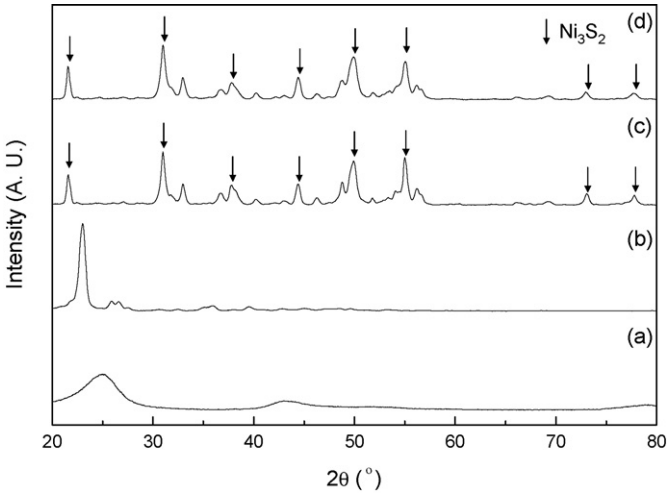

Fig. 2. XRD patterns of raw materials: (a) carbon, (b) PEO, (c) raw Ni_3S_2, and (d) Ni_3S_2 after ball-milling for 2 h.

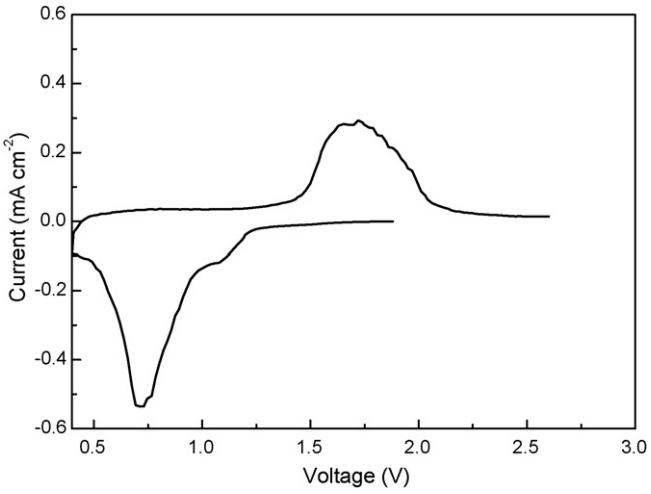

Fig. 3. Cycle voltammogram of Ni_3S_2 vs. Na at the room temperature.

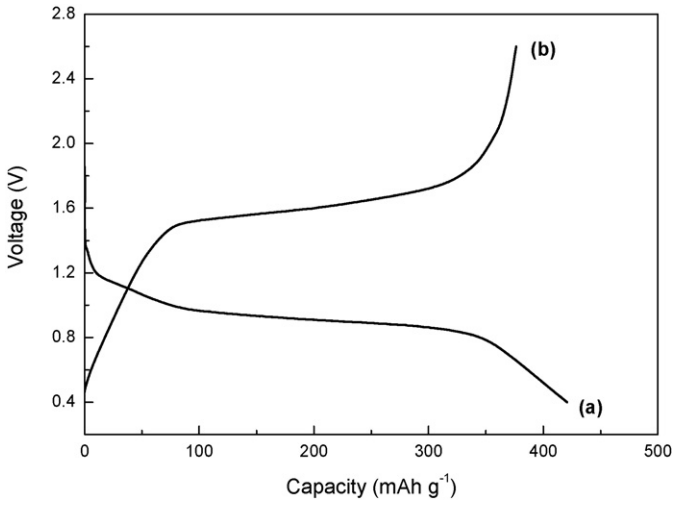

Fig. 4. First discharge–charge curve of Na/Ni_3S_2 cell with 50 mA g^{-1} at room temperature: (a) discharge and (b) charge reactions.

bohedral structure, which is stable structure of Ni_3S_2 at room temperature. After 2 h ball-milling of Ni_3S_2 powders, XRD pattern does not change, which means no structural change during ball-milling.

The cyclic voltammogram of the Na/Ni_3S_2 cell is given in Fig. 3. The potential sweep rate is 0.1 mV s^{-1} and the voltage range is from 2.6 to 0.4 V versus Na/Na^+ at ambient temperature. The system showed a large hysteresis in the oxidation and reduction processes due to the electrochemical reaction in Ni_3S_2. There exists a high current peak at 0.74 V during oxidation, which can suggest intercalation of sodium into Ni_3S_2, while there is a high current peak at 1.69 V during reduction due to deintercalation of sodium from the Ni_3S_2 phase.

Fig. 4 shows the first discharge–charge curve of the Na/Ni_3S_2 cell with a current density of 50 mA g^{-1} at ambient temperature. The first discharge curve has a potential plateau at 0.94 V and a high-specific discharge capacity of 420 mAh g^{-1}. The first charge curve has a specific capacity of 376 mAh g^{-1}, which shows a plateau potential at 1.62 V. This result is similar to the cyclic voltammogram curve in Fig. 3. Since this is the first report for a Na/Ni_3S_2 cell, it is impossible to compare with previous results. The Na/Ni_3S_2 cell has a lower discharge plateau potential than Li/Ni_3S_2 cells and first discharge capacity is similar to Li/Ni_3S_2 cells [8]. The discharge potential difference should come from the fact that standard reduction potential of sodium (−2.71 V) is higher than lithium (−3.01 V).

Fig. 5 shows the changes of SEM images for the Ni_3S_2 electrode during charge and discharge. The original Ni_3S_2 electrode represents a mixture of Ni_3S_2 powder and carbon black. After the first discharge, the electrode surface shows agglomerations. This phenomenon is similar to other Li/S and Li/sulfide cells [12,13]. Therefore it is assumed that sodium polysulfide might be dissolved in the electrolyte. The electrode surface after the first charge reaction is regenerated into the original shape.

Fig. 6 shows the change in XRD profiles of the Ni_3S_2 cathode during the electrochemical discharge–charge reaction. The XRD profile of the original Ni_3S_2 electrode shows Ni_3S_2 phases of a rhombohedral structure. After discharge reaction, the peaks of Ni_3S_2 phases disappear and then the new peaks of Na_2S and Ni are detected. It is suggested that Ni_3S_2 changes into Na_2S and pure Ni during discharge by Eq. (1). The Gibbs free energy of formation (ΔG_f) was obtained from JANAF Thermochemical Tables.

$$4Na + Ni_3S_2 \rightarrow 3Ni + 2Na_2S, \quad E_0 = 1.29\,V,$$
$$\Delta G(Na_2S) = -354.552\,kJ\,mol^{-1} \quad [14] \qquad (1)$$

The electromotive force (E_0) of a cell can be calculated from the Gibbs free energy of formation (ΔG_f) by the following equation:

$$\Delta G_f = -nFE_0 \qquad (2)$$

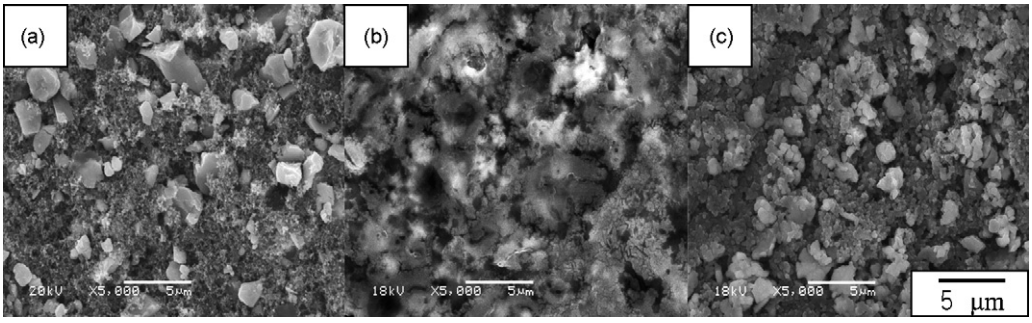

Fig. 5. SEM images of Ni_3S_2 electrodes: (a) original, (b) after 1st discharge, and (c) after 1st charge.

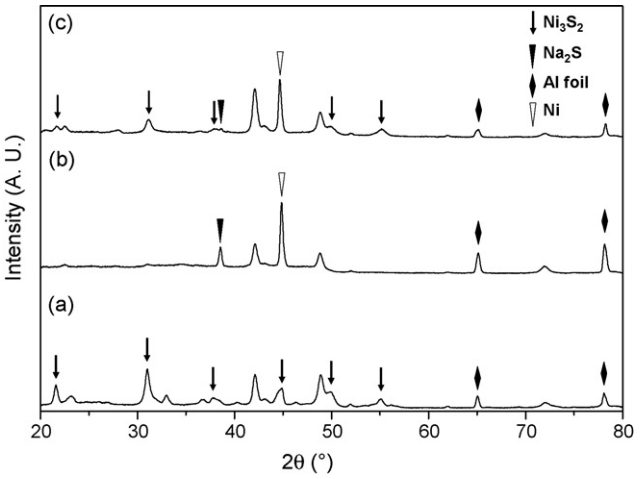

Fig. 6. XRD patterns of electrodes: (a) original, (b) after 1st discharge, and (c) after 1st charge.

where ΔG_f is the change of Gibbs free energy, n is the number of electrons involved in stoichiometric reaction, F is the Faraday's constant (96,487 C), and E_0 is the electromotive force.

The electromotive force of Na_2S is calculated into 1.29 V. The phase diagram between sodium and sulfur shows not only Na_2S, but also several compounds such as NaS, Na_2S_3, NaS_2, and Na_2S_5 [4]. Thus, the following reactions are possible during the discharge process of Ni_3S_2.

$$2Na + Ni_3S_2 \rightarrow 3Ni + Na_2S_2, \quad E_0 = 0.94\,V,$$
$$\Delta G(Na_2S_2) = -210.399\,kJ\,mol^{-1} \quad [14] \qquad (3)$$

$$4Na + 3Ni_3S_2 \rightarrow 9Ni + 2Na_2S_3, \quad E_0 = 0.46\,V,$$
$$\Delta G(Na_2S_3) = -354.552\,kJ\,mol^{-1} \quad [4] \qquad (4)$$

The electromotive forces (E_0) of Na_2S, Na_2S_2, and Na_2S_3 are 1.29, 0.94, and 0.46 V, respectively. The thermodynamic standard electromotive force (E_0) should exist between charge plateau (1.62 V) and discharge plateau (0.94 V). From the thermodynamic point, the formation of Na_2S_3 (Eq. (4)) cannot explain the discharge–charge process shown in Fig. 4. The theoretical specific capacities of Na_2S, Na_2S_2, and Na_2S_3 are 446, 223, and 149 mAh g^{-1} based on the above Eqs. (1), (3) and (4), respectively. The theoretical specific capacity of Na_2S_2 (223 mAh g^{-1}) product by Eq. (3) is too small to explain the first discharge capacity (420 mAh g^{-1}) of Fig. 4. The plateau potential of 0.94 V and 420 mAh g^{-1} shown in Fig. 4 can be explained only by the formation of Na_2S corresponding with Eq. (1) at ambient temperature, which coincided with the XRD result shown in Fig. 6. Although high-temperature Na/S cells formed the Na_2S_3 or Na_2S_5 phases, the discharge process of the Na/Ni_3S_2 cell at room temperature is related to the formation of Na_2S. If nickel sulfide (Ni_3S_2) is recovered reversibly during the charge reaction at room temperature, the following reaction (Eq. (5)), the reverse reaction of Eq. (1), should be occurred during charging process:

$$2Na_2S + 3Ni \rightarrow Ni_3S_2 + 4Na \qquad (5)$$

However, the XRD profile after charge shows peaks of Ni_3S_2 in addition to Na_2S and Ni phases. Although Na_2S and Ni are changed into Ni_3S_2 during the charge reaction, all of Ni_3S_2 component cannot be recovered by Eq. (5). Some of Na_2S and Ni phase remain after charge.

In order to investigate irreversible process of a charge reaction, elemental mapping data of the Ni_3S_2 electrode after the first charge reaction are shown in Fig. 7. The bright regions are composed of sulfur, nickel, and sodium components. Nickel and sulfur can be detected in every region of the Ni_3S_2 elec-

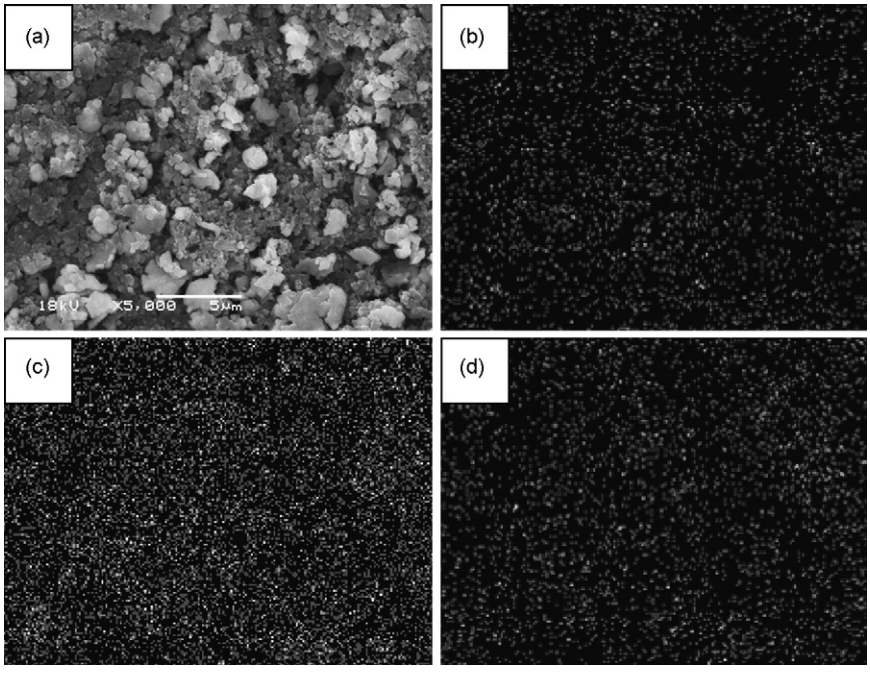

Fig. 7. SEM image and elemental mapping of Ni_3S_2 electrode after 1st charge: (a) SEM image and elemental mapping of (b) sodium, (c) sulfur, and (d) nickel.

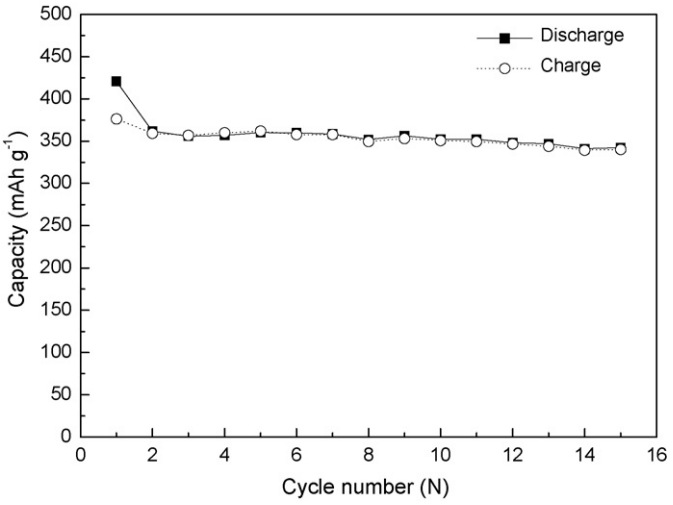

Fig. 8. Cycle performance of Na/Ni_3S_2 cell at room temperature.

trode, which might come from Ni_3S_2, Na_2S, and Ni phases shown in Fig. 6. Also, the sodium component still remains in the Ni_3S_2 electrode after charging, which can be related to small peaks of Na_2S shown in Fig. 6. During the charge process, some Na_2S and Ni transform to Ni_3S_2 but the rest still remains as Na_2S and Ni in the Ni_3S_2 electrode. Since Na_2S is already fully reduced, it cannot reduce anymore during discharge process. Thus remaining Na_2S led to capacity loss. Therefore the following reactions might be possible during the charge process of Ni_3S_2.

$$2Na_2S + 3Ni \rightarrow xNi_3S_2 + 4xNa + (1-x)Na_2S + 3(1-x)Ni \quad (6)$$

Fig. 8 shows the repeated charge and discharge cycles of the Na/Ni_3S_2 cell. The second discharge cycle shows a capacity loss of 60 mAh g^{-1} compared to the initial capacity. The discharge capacity is maintained at about 342 mAh g^{-1}, which retains 81% of its initial discharge capacity until 15 cycles. While batteries such as Na/S and Na/FeS_2 had shown poor cycle properties, the Na/Ni_3S_2 cell in Fig. 8 shows a good cycle property during the several cycles [6,7,15]. Li/NiS and Li/Ni_3S_2 cells have had a long cycle life. Moreover, the Na/Ni_3S_2 cell shows a very stable property in terms of cycle performance. Therefore, it is considered that nickel sulfides such as NiS and Ni_3S_2 are the suitable materials among promising cathode materials.

4. Conclusions

The charge–discharge characteristics of a sodium/nickel sulfide (Ni_3S_2) cell have been investigated at room temperature. A Na/Ni_3S_2 cell gives a high initial discharge capacity of 420 mAh g^{-1} with a plateau potential region at 0.94 V versus Na/Na^+ at ambient temperature and also shows good cycle performance over 15 cycles. The discharge process can be explained; $Ni_3S_2 + 4Na \leftrightarrow 3Ni + 2Na_2S$. However, some of the Na_2S component still remains in the Ni_3S_2 cathode after charge reaction. Ni_3S_2 could be a promising candidate as a cathode material for sodium batteries at room temperature.

Acknowledgements

This research was supported by the MIC (Ministry of Information and Communication), Republic of Korea, under the ITRC (Information Technology Research Center) support program supervised by IITA (Institute of Information Technology Assessment).

References

[1] N. Sato, J. Power Sources 99 (2001) 70–77.
[2] K. Smith, C.Y. Wang, J. Power Sources 160 (2006) 662–673.
[3] R. Okuyama, J. Nakashima, T. Sano, E. Nomura, J. Power Sources 97 (2001) 50–54.
[4] J.L. Sudworth, A.R. Tilley, The Sodium Sulfur Battery, Chapman & Hall, New York, 1985.
[5] J. Wang, J. Yang, Y. Nuli, R. Holze, Electrochem. Commun. 9 (2007) 31–34.
[6] C.W. Park, H.S. Ryu, K.W. Kim, J.H. Ahn, J.Y. Lee, H.J. Ahn, J. Power Sources 165 (2007) 450–454.
[7] C.W. Park, J.H. Ahn, H.S. Ryu, K.W. Kim, H.J. Ahn, Electrochem. Solid State Lett. 9 (2006) A123–A125.
[8] X. Zhu, Z. Wen, Z. Gu, S. Huang, J. Electrochem. Soc. 153 (2006) A504–A507.
[9] S.C. Han, H.S. Kim, M.S. Song, P.S. Lee, J.Y. Lee, H.J. Ahn, J. Alloys Compd. 349 (2003) 290–296.
[10] S.C. Han, K.W. Kim, H.J. Ahn, J.H. Ahn, J.Y. Lee, J. Alloys Compd. 361 (2003) 247–251.
[11] R. Jasinski, B. Burrows, J. Electrochem. Soc. 116 (1969) 422–424.
[12] J.S. Chung, H.J. Sohn, J. Power Sources 108 (2002) 226–231.
[13] L.X. Yuan, J.K. Feng, X.P. Ai, Y.L. Cao, S.L. Chen, H.X. Yang, Electrochem. Commun. 8 (2006) 610–614.
[14] M.W. Chase, C.A. Davies, J.R. Downey, D.J. Frurip, R.A. McDonald, A.N. Syverud, JANAF Thermochemical Tables, 3rd ed., American Institute of Physics, American Chemical Society and the American Institute of Physics for the National Bureau of Standards, 1985, pp. 1595, 1598, 1635.
[15] T.B. Kim, W.H. Jung, H.S. Ryu, K.W. Kim, J.H. Ahn, K.K. Cho, G.B. Cho, T.H. Nam, I.S. Ahn, H.J. Ahn, J. Alloys Compd. 449 (2008) 304–307.